

# OPTIMAL ANGLE BOUNDS FOR QUADRILATERAL MESHES

CHRISTOPHER J. BISHOP

ABSTRACT. We show that any simple planar  $n$ -gon can be meshed in linear time by  $O(n)$  quadrilaterals with all new angles bounded between 60 and 120 degrees.

---

1991 *Mathematics Subject Classification.* Primary: 30C62 Secondary:

*Key words and phrases.* Quadrilateral meshes, Riemann mapping, thick/thin decomposition, linear time.

The author is partially supported by NSF Grant DMS 04-05578.

## 1. INTRODUCTION

We answer a question of Bern and Eppstein by proving:

**Theorem 1.1.** *Any simply connected planar domain  $\Omega$  whose boundary is a simple  $n$ -gon has a quadrilateral mesh with  $O(n)$  pieces so that all angles are between  $60^\circ$  and  $120^\circ$ , except that original angles of the polygon with angle  $< 60^\circ$  remain. The mesh can be constructed in time  $O(n)$ .*

The theorem is sharp in the sense that no shorter interval of angles suffices for all polygons: using Euler’s formula, Bern and Eppstein proved (Theorem 5 of [2]) that any quadrilateral mesh of a polygon with all angles  $\geq 120^\circ$  must contain an angle  $\geq 120^\circ$ . On the other hand, any boundary angle  $\theta > 120^\circ$  must be subdivided by the mesh in Theorem 1.1 and hence there must be a new angle  $\leq \theta/2$  in the mesh. Thus taking polygons with an angle  $\theta \searrow 120^\circ$  shows  $60^\circ$  is the optimal lower bound.

It is perhaps best to think of Theorem 1.1 as an existence result. Although we give a linear time algorithm for finding the mesh, the constant is large and the construction depends on other linear algorithms, such Chazelle’s linear time triangulation of polygons, that have not been implemented (as far as I know).

The three main tools in the proof of Theorem 1.1 are conformal maps, thick/thin decompositions of polygons and hyperbolic tessellations. We will decompose  $\Omega$  into  $O(n)$  “thick” and “thin” parts. The thin parts have simple shapes and we can easily construct an explicit mesh in each of them. The thick parts are more complicated, but we can use a conformal map to transfer a mesh from the unit disk,  $\mathbb{D}$ , to the thick parts of  $\Omega$  with small distortion. The mesh on  $\mathbb{D}$  is produced using a finite piece of an infinite tessellation of  $\mathbb{D}$  by hyperbolic pentagons.

I would like to thank Marshall Bern for asking me the question that lead to Theorem 1.1 and pointing out his paper [2] with David Eppstein. Also thanks to Joe Mitchell for many helpful conversations on computational geometry. This paper is part of a series ([3], [4], [5], [6]) that exploits the close connection between the medial axis of a planar domain, the geometry of its hyperbolic convex hull in  $\mathbb{H}_+^3$  and the conformal map of the domain to the disk. This was originally motivated by a result of Dennis Sullivan [15] about boundaries of hyperbolic 3-manifolds and its generalization by David Epstein (only one “p” this time) and Al Marden [9]. Many thanks to those

authors for the inspiration and insights they have provided. Also many thanks to the referees for a careful reading of the original manuscript. Their thoughtful comments and suggestions greatly improved the paper. One of them pointed out reference [11] where the Riemann mapping theorem is used to prove that any polygon with all angles  $\geq \pi/5$  can be dissected into triangles with all angles  $\leq 2\pi/5$ .

## 2. MÖBIUS TRANSFORMATIONS AND HYPERBOLIC GEOMETRY

A linear fractional (or Möbius) transformation is a map of the form  $z \rightarrow (az + b)/(cz + d)$ . This is a 1-1, onto, holomorphic map of the Riemann sphere  $S^2 = \mathbb{C} \cup \{\infty\}$  to itself. Such maps form a group under composition and are well known to map circles to circles (if we count straight lines as circles that pass through  $\infty$ ). Möbius transforms are conformal, so they preserve angles. Given two sets of distinct points  $\{z_1, z_2, z_3\}$  and  $\{w_1, w_2, w_3\}$  there is a unique Möbius transformation that sends  $w_k \rightarrow z_k$  for  $k = 1, 2, 3$ . A Möbius transformation maps the unit disk,  $\mathbb{D}$ , to itself iff it is of the form  $g(z) = \lambda(z - a)/(1 - \bar{a}z)$  for some  $a \in \mathbb{D}$ ,  $|\lambda| = 1$ .

The hyperbolic metric on the unit disk is given by

$$\rho(v, w) = \inf_{\gamma} \int_{\gamma} \frac{2|dz|}{1 - |z|^2},$$

where the infimum is over all rectifiable arcs connecting  $v$  and  $w$  in  $\mathbb{D}$ . This is a metric of constant negative curvature. In some sources, the “2” is omitted; we have chosen this version to be consistent with the trigonometric formulas found in [1]. Geodesics for this metric are circular arcs that are perpendicular to the boundary (including diameters). Hyperbolic area is given by  $4dxdy/(1 - |z|^2)^2$ . The area of a triangle with geodesic edges is  $\pi - \alpha - \beta - \gamma$ , where  $\alpha, \beta, \gamma$  are the interior angles. Thus the area of any hyperbolic triangle is  $\leq \pi$ .

The hyperbolic metric is well known to be invariant under Möbius transformations of the disk, so it is enough to compute it when one point has been normalized to be 0 and the other rotated to the positive axis. If  $0 < x < 1$  and  $\rho = \rho(0, x)$ , then

$$\rho = \log \frac{1+x}{1-x}, \quad x = \frac{e^{\rho} - 1}{e^{\rho} + 1}.$$

It is also convenient to consider the isometric model of the upper half-space,  $\mathbb{H}$ . In this case the hyperbolic metric is given by

$$\rho(v, w) = \inf \int_{\gamma} \frac{|dz|}{y},$$

where  $z = x + iy$ , but geodesics are still circular arcs perpendicular to the boundary.

If  $E \subset \mathbb{T} = \partial\mathbb{D}$  is closed then  $\mathbb{T} \setminus E = \cup I_j$  is a union of open intervals. The hyperbolic convex hull of  $E$ , denoted  $\text{CH}(E)$ , is the region in  $\mathbb{D}$  bounded by  $E$  and the collection of circular arcs  $\{\gamma_j\}$ , where  $\gamma_j$  is the hyperbolic geodesic with the same endpoints as  $I_j$ . See Figure 1.

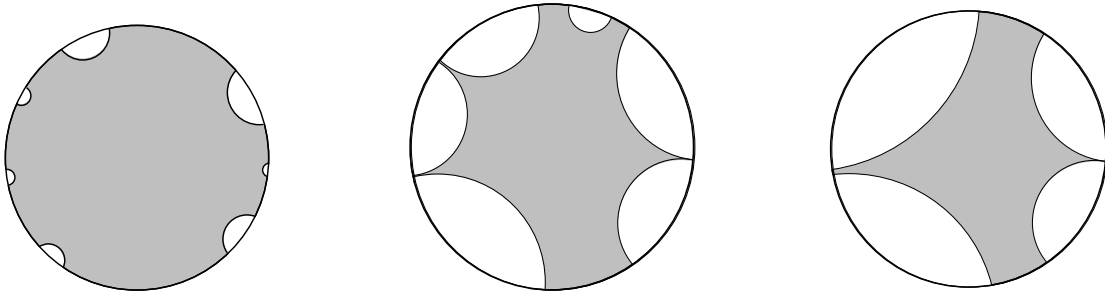


FIGURE 1. Examples of hyperbolic convex hulls. The one on the left is uniformly perfect, the center is thick with a large  $\eta$ , but not uniformly perfect, and the right is only thick with a small  $\eta$  (there are two geodesics that almost touch, but do not share an endpoint).

A closed set  $E \subset \mathbb{T}$  is called  $\eta$ -thick if any two components of  $\partial\text{CH}(E) \cap \mathbb{D}$  that don't share an endpoint are at least hyperbolic distance  $\eta$  apart. If  $E$  is  $\eta$ -thick, then any point in the hull is contained in a hyperbolic ball of radius  $\eta$  that is also contained in the convex hull. The thickness condition can be written in other ways. For example,  $E$  is  $\eta$ -thick iff non-adjacent complementary intervals have extremal distance at least  $\delta > 0$  (with  $\delta^{-1} \simeq \frac{2}{\pi} \log \frac{1}{\eta}$  for small  $\delta, \eta$ ) [6]. A closed set  $E$  is called uniformly perfect if any two components of  $\partial\text{CH}(E) \cap \mathbb{D}$  are at least hyperbolic distance  $\eta$  part. This stronger condition arises many places in function theory, but will not be used in this paper.

## 3. A SUBDIVISION OF THE HYPERBOLIC DISK

To prove Theorem 1.1 we will divide the interior of  $\Omega$  into pieces called “thick” and “thin” (see [6] and Section 7). The thin pieces will be meshed explicitly, but the mesh on the thick pieces will be transferred from a quadrilateral mesh of a domain in the unit disk via a conformal map. Most of our time will be spent constructing the mesh on the disk. In this section we describe the subdomain and how to subdivide it into circular arc triangles, quadrilaterals and pentagons. In the following sections we show how to construct quadrilateral meshes for each subregions that are consistent along shared boundaries.

A compact hyperbolic polygon is a bounded region in hyperbolic space bounded by a finite number geodesic segments. The polygon is “right” if every interior angle is  $90^\circ$ . There are no compact hyperbolic right triangles or quadrilaterals, but there are hyperbolic right  $n$ -gons for every  $n \geq 5$  and any such can be extended to a tessellation  $\mathcal{T}_n$  of hyperbolic space by repeated reflections. See Figure 2 for the case of pentagons (the only case we use in this paper).

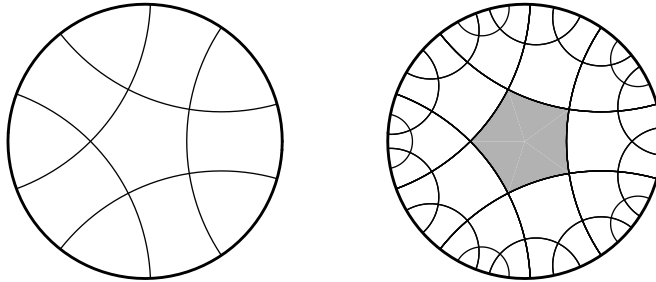


FIGURE 2. A hyperbolic right pentagon (left) and the its neighbors in the tessellation  $\mathcal{T}_5$ .

Let  $L \approx 1.6169$  denote the side length of a hyperbolic right pentagon. We don’t need the specific value, but it can be computed using  $\gamma = \pi/5$ ,  $\alpha = \beta = \pi/4$  in the second hyperbolic law of cosines (see [1]):

$$\cosh c = \frac{\cos \alpha \cos \beta + \cos \gamma}{\sin \alpha \sin \beta}.$$

In the tessellation  $\mathcal{T}_5$ , each edge of a pentagon lies on some hyperbolic geodesic. Each of these geodesics divides  $\mathbb{T}$  into two arcs and we let  $\mathcal{I}_5$  denote the collection of all such arcs.

**Lemma 3.1.** *There is a  $c < \infty$  so that given any arc  $J \subset \mathbb{T}$  there are  $I_1, I_2 \in \mathcal{I}_5$  with  $I_1 \subset J \subset I_2$  and  $|I_2|/|I_1| \leq c$  ( $|\cdot|$  denotes arclength).*

*Proof.* Let  $\gamma$  be the hyperbolic geodesic with the same endpoints as  $J$ . The top point of  $\gamma$  (i.e., the point closest to 0) is contained in some pentagon of the tessellation. By taking  $c$  larger, we can assume  $J$  is as short as we wish, so we may assume this is not the central pentagon. Let  $a$  be the hyperbolic center of this pentagon and let  $g(z) = \lambda(z - a)/(1 - \bar{a}z)$  where  $|\lambda| = 1$  is chosen  $g$  maps the pentagon to the central pentagon. This is a Möbius transformation that sends  $a$  to 0, maps the diameter  $D$  through  $a$  into  $\lambda D$  and maps  $\gamma$  to a geodesic  $\gamma'$  that intersects the central pentagon of the tessellation. Moreover, since  $g$  preserves angles, the angle between  $\gamma'$  and  $D' = \lambda D$  is the same as between  $\gamma$  and  $D$ , and this is bounded away from 0, since the intersection point is within distance  $L$  of the top point of  $\gamma$ .

Thus  $\gamma'$  also makes a large angle with  $D'$  and so is some positive distance  $r$  from the point  $b = -\lambda a = g(0)$ . The inverse of  $g$  is  $f(z) = \bar{\lambda}(z - b)/(1 - \bar{b}z)$  and the derivative of this is  $(1 - |b|^2)/(1 - \bar{b}z)^2$ . From this we see that for  $|z| = 1$ ,

$$\frac{1 - |b|}{|z - b|^2} \leq |f'(z)| \leq \frac{2(1 - |b|)}{|z - b|^2},$$

so that  $|f'(z)| \simeq 2(1 - |b|)$  with a constant that depends only on  $|z - b|$ . Thus sets outside a ball around  $b$  will be compressed similar amounts by  $f$ .

Choose geodesics  $\gamma_1, \gamma_2$  from the tessellation edges on either side of  $\gamma'$  so that  $\gamma_1$  separates  $b$  from  $\gamma'$  and has a uniformly bounded distance  $r$  from  $b$  (we can easily do this if  $1 - |b| = 1 - |z| \simeq |J|$  is small enough). Apply  $f$  to  $\gamma_1, \gamma_2$  and we get two geodesics of comparable Euclidean size whose base intervals are the desired  $I_1, I_2$ .  $\square$

A Carleson triangle in  $\mathbb{D}$  is a region bounded by two geodesic rays that have a common endpoint where they meet with interior angle  $90^\circ$ . Any two such are Möbius equivalent. A Carleson quadrilateral is bounded by one finite length hyperbolic segment and two geodesic rays, again with both interior angles equal  $90^\circ$ . See Figure 3. It is determined up to isometry by the hyperbolic length of its finite length edge. In this paper all of our Carleson quadrilaterals will have length  $L$ , where  $L$  is the side length of a right pentagon, as above.

We will prove the following:

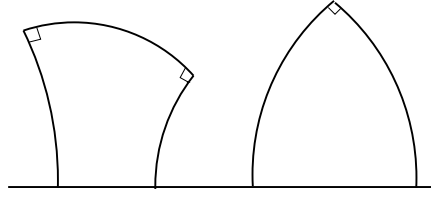


FIGURE 3. A Carleson quadrilateral and triangle.

**Lemma 3.2.** *There is a  $c < \infty$  so that the following holds. Suppose we are given  $A > 1$  and a finite collection intervals  $\{I_j\}_1^N$  on the unit circle so that the expanded intervals  $\{AI_j\}$  are disjoint (these are the concentric intervals that are  $A$  times longer) and each has length  $< \pi$ . Let  $E = \cup_j I_j$ . We can find intervals  $\{J_j\}$  so that*

- (1)  $\sqrt{AI_j} \subset J_j \subset c\sqrt{AI_j}$ ,  $j = 1, \dots, N$ .
- (2) *Let  $F = \cup_j J_j$  and let  $W \subset \mathbb{D}$  be the hyperbolic convex hull of  $\mathbb{T} \setminus F$ . Then  $W$  has a mesh  $\{W_k\}$  consisting of right hyperbolic pentagons, Carleson quadrilaterals and Carleson triangles. A pentagon shares an edge only with other pentagons or the top of a quadrilateral, a quadrilateral shares a top edge only with pentagons and side edges with triangles and other quadrilaterals, and a triangle shares edges only with quadrilaterals.*
- (3) *Each component of  $\partial W \cap \mathbb{D}$  is an infinite geodesic that is the union of side edges from two Carleson quadrilaterals and edges from three pentagons.*
- (4) *Every pentagon used in the mesh is a uniformly bounded hyperbolic distance from the hyperbolic convex hull of  $E$ .*
- (5) *Every region  $W_k$  in the mesh has diameter bounded by  $O(\text{dist}(W_k, E))$  (Euclidean distances).*

*Proof.* For each interval  $I_j$  given in the lemma, choose  $J_j \in \mathcal{I}_5$  to be the minimal interval containing  $\sqrt{AI_j}$ . Then (1) clearly holds by Lemma 3.1.

Let  $\gamma_j$  be the geodesic with the same endpoints as  $J_j$  and let  $P_0$  be a pentagon in  $\mathcal{T}_5$  that is above  $\gamma_j$  (i.e, whose interior lies in the component of  $\mathbb{D} \setminus \gamma_j$  containing 0) and whose boundary contains the “top” of  $\gamma_j$  (the point closest to 0). Let  $P_1, P_2$  be the elements of  $\mathcal{T}_5$  that are adjacent to  $P_0$  and also above  $\gamma_j$ . Then the part of  $\gamma_j$  covered by the boundaries of these three pentagons contains an interval of hyperbolic length  $2L$  centered at the top point. Let  $\gamma_j^1$  be the geodesic containing the side of  $P_1$  that has one endpoint on  $\gamma_j$  and is not on  $\partial P_0$ . Let  $J_j^1 \in \mathcal{I}_5$  be the base interval of

$\gamma_j^1$ . Let  $J_j^2 \in \mathcal{I}_5$  be the corresponding interval for  $P_2$  and let  $J'_j = J_j^1 \cup J_j \cup J_j^2$ . See Figure 4.

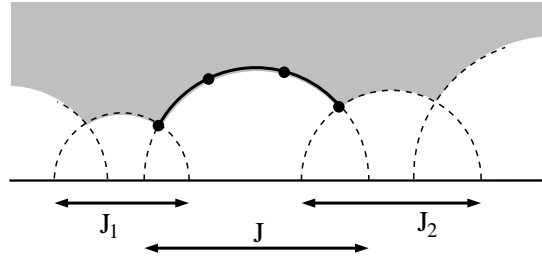


FIGURE 4. On the left are  $J, J_1, J_2$ . The shaded region is a union of the pentagons; the white is a union of quadrilaterals and triangles.

Let  $G = \cup_j (J_j^1 \cup J_j \cup J_j^2)$  and let  $\{\mathcal{K}\}$  be the collection of intervals in  $\mathcal{I}_5$  that are compactly contained in  $\mathbb{T} \setminus F$ , contain a point of  $\mathbb{T} \setminus G$  and are maximal in the sense of containment with respect to these properties. These clearly cover all of  $\mathbb{T} \setminus G$ . Now add the intervals  $J_j, J_j^1, J_j^2$  to get a cover of the whole circle. Any open finite cover of an interval has a subcover with overlaps of at most 2 (if a point is in three intervals we can keep the ones with leftmost left endpoint and rightmost right endpoint and throw away the third; repeat until every point is in at most two intervals). For such a subcover, we mesh  $W$  with pentagons above the corresponding geodesics and by Carleson quadrilaterals and triangles below. See Figure 5. Conditions (2) and (3) are clear from construction.

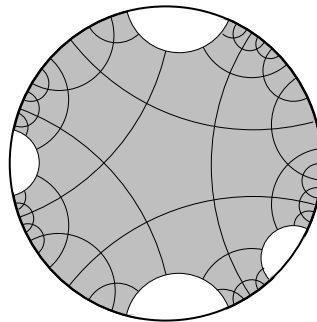


FIGURE 5. An example of meshing a convex hull  $W$  with pentagons, quadrilaterals and triangles. This example is not to scale, since the white regions should be much smaller than their distances apart.

If  $x \in \mathbb{T} \setminus F$  and  $d = \text{dist}(x, F)$  then apply Lemma 3.1 to an interval of length  $\frac{1}{2}d/c$  centered at  $x$ . We obtain an element of  $\mathcal{I}_5$  containing  $x$ , missing  $F$  and of length  $\geq \frac{1}{2}d/c$ . Thus the maximal interval of  $\mathcal{K}$  containing  $x$  has at least this length. This implies (4).

Every right pentagon  $P$  has Euclidean diameter bounded by  $O(\text{dist}(P, \mathbb{T})) = O(\text{dist}(P, E))$ . Every Carleson quadrilateral  $R$  has a top edge along a geodesic  $\gamma$  with endpoints  $\{a, b\}$  and  $\text{diam}(R) \simeq \text{dist}(R, \{a, b\})$ . Since  $\gamma$  misses the hyperbolic convex hull of  $E$ , the latter is  $\leq \text{dist}(Q, R)$ . Every Carleson triangle is adjacent to two Carleson quadrilaterals of comparable Euclidean size that separate it from  $E$ , so the estimate also holds for these triangles. Thus (5) holds.  $\square$

**Lemma 3.3.** *If the collection  $\{I_j\}_1^n$  satisfies the conditions of Lemma 3.2 and if, in addition, the set  $E = \cup_j I_j$  is a  $\delta$ -thick set, then the mesh constructed in Lemma 3.2 has  $O(n)$  elements, with a constant that depends only on  $\delta$ .*

*Proof.* Choose a disjoint collection of  $\eta$ -balls in  $S = \text{CH}(E) \cap W$  and note that there are  $O(n)$  such balls since  $S$  has hyperbolic area  $O(n)$  (it is a convex hyperbolic polygon with  $O(n)$  sides, hence has a triangulation into  $O(n)$  hyperbolic triangles, and every hyperbolic triangle has hyperbolic area  $\leq \pi$ ).

Every pentagon used in the proof of Lemma 3.2 is within a bounded hyperbolic distance  $D$  of one of the chosen  $\eta$ -balls, so only  $O(1)$  pentagons can be associated to any one ball (they are disjoint, have a fixed area and all lie in a ball of fixed radius, hence fixed area). Thus the total number of pentagons used is  $O(n)$ . Every Carleson quadrilateral shares an edge with a pentagon and every Carleson triangle shares an edge with a quadrilateral, so the number of these regions is also  $O(n)$ .  $\square$

#### 4. MESHING THE PENTAGONS

In the last section we subdivided the unit disk into hyperbolic pentagons, quadrilaterals and triangles. Next we want to mesh each of these regions into quadrilaterals with angles in the interval  $[60^\circ, 120^\circ]$ . Moreover, along common edges of the regions, the vertices of the meshes must match up correctly.

For each type of region, we will produce a mesh by quadrilaterals that have circular arc boundaries and angles within a given range. In most cases the boundary arcs lie on circles with radius comparable to the region, and the quadrilaterals will be much

smaller, about  $1/N$  as large, for a large  $N$ . If we replace the circular arc edges by line segments, the angles change by only  $O(1/N)$ , which still gives angles in the desired range. The only exceptions will be certain parts of the mesh of the Carleson triangles, that will require a separate argument to show the “snap-to-a-line” angles are still between  $60^\circ$  and  $120^\circ$ .

As before,  $L$  denotes the sidelength of a hyperbolic right pentagon.

**Lemma 4.1.** *For sufficiently large integers  $N > 0$  the following holds. Suppose  $P$  is a hyperbolic right pentagon. Then there is mesh of  $P$  into hyperbolic quadrilaterals with angles between  $72^\circ$  and  $108^\circ$ . The mesh divides each side of the pentagon into  $N$  segments of length  $L/N$ . Each quadrilateral  $Q$  in the mesh has hyperbolic diameter  $O(1/N)$  and satisfies  $\text{diam}(Q) = O(\frac{1}{N} \cdot \text{diam}(P))$  in the Euclidean metric. Replacing the edges of  $Q$  by line segments changes angles by only  $O(1/N)$ .*

*Proof.* Connect the center  $c$  of the pentagon by hyperbolic geodesics to the (hyperbolic) center of each edge. This divides the pentagon into five quadrilaterals each of which has 3 right angles and an angle of  $72^\circ$  at the center. Consider one of these quadrilaterals  $Q$  with sides  $S_1, S_2, S_3, S_4$  where  $S_1, S_2$  each connects the center of the pentagon to midpoints of adjacent sides. Then  $S_3, S_4$  are each half of a side of the pentagon adjacent at a vertex  $v$ , with  $S_3$  opposite  $S_1$  and  $S_4$  opposite  $S_2$  (Figure 6).

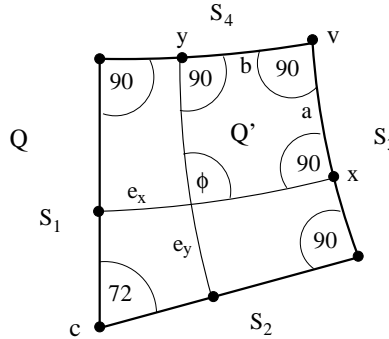


FIGURE 6. Definitions used in the mesh of a hyperbolic right pentagon. Each pentagon is divided into five quadrilaterals as shown.

Place a point  $x$  along  $S_3$  and let  $e_x$  be the geodesic segment from  $S_1$  to  $S_3$  that meets  $S_3$  at  $x$  and makes a  $90^\circ$  angle with  $S_3$ . Similarly define a segment  $f_y$  that joints  $y \in S_4$  to  $S_2$ . We claim that the segments cross at an angle (labeled  $\phi$  in Figure 6) that

is between  $72^\circ$  and  $90^\circ$ . The two segments  $e_x, f_y$  divide  $Q$  into four quadrilaterals, one of which contains the vertex  $v$ . This subquadrilateral,  $Q'$  is a Lambert quadrilateral, i.e., bounded by four hyperbolic geodesic segments and having 3 right angles. The one non-right angle,  $\phi$ , is a function of the hyperbolic lengths of the two opposite sides (in this case a function of  $a = \rho(x, v)$  and  $b = \rho(y, v)$ ),

$$\cos(\phi) = \sinh a \sinh b.$$

See Theorem 7.17.1 of [1]. Clearly,  $\phi$  decreases as either  $a$  or  $b$  increase. For  $a$  and  $b$  close to zero we have  $\phi \approx 90^\circ$  and when  $a, b$  take their maximum value ( $a = b$  is the hyperbolic length of  $S_3$ ) we get  $Q' = Q$  and  $\phi = 72^\circ$ . Thus  $\phi$  takes values between  $72^\circ$  and  $90^\circ$ , as claimed.

To define a mesh of  $Q$ , take  $N$  equally spaced points  $\{x_k\} \subset S_3$  and  $\{y_k\} \subset S_4$  and take the union of segments  $e_{x_k}, f_{y_k}$ . This divides  $Q$  into quadrilaterals with geodesic boundaries and angles between  $72^\circ$  and  $108^\circ$ . Doing this for each of the five quadrilaterals that make up the hyperbolic right pentagon gives a mesh of the pentagon. The remaining claims are easy to verify. See Figure 7.

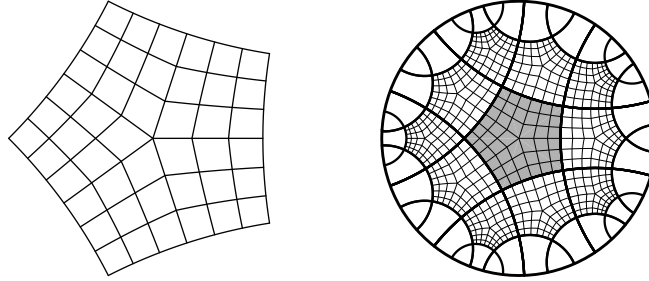


FIGURE 7. A quadrilateral mesh of a single pentagon and the mesh on 11 adjoining pentagons. Because vertices are evenly spaced in the hyperbolic metric, meshing of adjacent pentagons match up.

□

## 5. MESHING THE QUADRILATERALS

**Lemma 5.1.** *For sufficiently large integers  $N$  the following holds. Suppose  $\{d_1 < d_2 < \dots < d_M\}$  satisfy  $|d_k - d_{k+1}| \leq 1/N$  for  $k = 1, \dots, M - 1$ ,  $d_1 < 1/N$ ,  $d_M > N$  and suppose  $R$  is a right Carleson quadrilateral. Then there is mesh of  $R$  into hyperbolic quadrilaterals with angles between  $90^\circ - O(\frac{1}{N})$  and  $90^\circ + O(\frac{1}{N})$ . The mesh*

divides the unique finite (hyperbolic) length side of  $R$  into  $N$  segments of length  $L/N$ . Each infinite length side of  $R$  has vertices exactly at the points that are hyperbolic distance  $d_k$ ,  $k = 1, \dots, m$  from the finite length side. If the base of  $R$  has length  $\leq \pi$ , then each element  $Q$  of the mesh satisfies  $\text{diam}(Q) = O(\frac{1}{N} \cdot \text{diam}(R))$  in the Euclidean metric. Replacing the edges of  $Q$  by lines segments changes angles by at most  $O(1/N)$ .

We need a simple preliminary result.

**Lemma 5.2.** *Suppose  $Q$  is a right circular quadrilateral, i.e., is bounded by four circular arcs and all four interior angles are  $90^\circ$ . Then  $Q$  has two orthogonal foliations by circular arcs. Every leaf of both foliations is perpendicular to the boundary at both of its endpoints.*

*Proof.* To see this, take two opposite sides. Each lies on a circle and these circles either intersect in 0, 1 or 2 points or are the same circle. In the first case we can conjugate by a Möbius transformation so both disks are centered at 0. Then the two other sides must map to radial segments and the foliations are as claimed. If the circles intersect in two points, we can assume these points are 0 and  $\infty$  so the circles are both lines passing through 0 and again the foliations are radial rays and circles centered at 0. If the opposite sides belong to the same circle, we can conjugate it to be the real line, with the two sides being arcs symmetric with respect to the origin. Then the other two sides must be circular arcs centered at 0 and the two foliations are as before. The last, and exceptional, case is if the two circles intersect in one point. Then we can conjugate this point to infinity and the intersecting sides to two parallel lines. The other two sides must map to perpendicular segments and the region is foliated by perpendicular straight lines. See Figure 8.  $\square$

*Proof of Lemma 5.1.* The two sides of  $R$  that lie in  $\mathbb{D}$  but have infinite hyperbolic length are geodesic rays that are both perpendicular to the geodesic containing the top edge of  $R$ . Hence they are subarcs of non-intersecting circles (to see this, isometrically map  $\mathbb{D} \rightarrow \mathbb{H}$  so the top edge maps to a vertical segment and the geodesic rays map to arcs of concentric circles). The foliations provided by the previous lemma consist of (1) hyperbolic geodesics that are perpendicular to the top edge of  $R$  (the unique finite length side) and (2) subarcs of circles that all pass through  $a, b$  (the endpoints

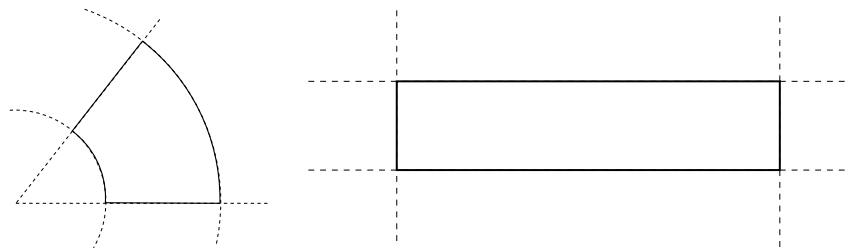


FIGURE 8. Any right circular quadrilateral is Möbius equivalent to one of these cases and hence has an orthogonal foliations by circular arcs.

of the hyperbolic geodesic that contains the top edge of  $R$ ). We call these the vertical and horizontal foliations respectively.

To prove the lemma, we simply subdivide the edges of  $R$  as described and take the foliation leaves with these endpoints. The only point that needs to be checked is that points on the two infinite length sides of  $R$  that are the same hyperbolic distance from the top edge lie on the same horizontal foliation leaf. However, any two horizontal leaves are equidistant from each other in the hyperbolic metric (to see this, map the vertices  $a, b$  to  $0, \infty$  by an isometry  $\mathbb{D} \rightarrow \mathbb{H}$  and these leaves become rays, and the claim is obvious since dilation is an isometry on  $\mathbb{H}$ ). Since the top edge is a horizontal leaf, we are done. See Figure 9.

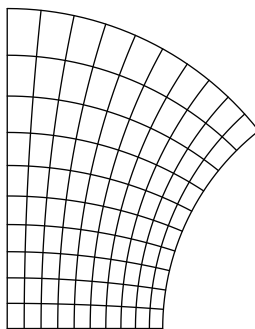


FIGURE 9. A quadrilateral mesh of a Carleson quadrilateral. “Horizontal” edges lie on circles that pass through the same two points on the boundary (the endpoints of the geodesic contain the top edge). “Vertical” edges are hyperbolic geodesics perpendicular to the top edge.

□

6. MESHING THE TRIANGLES

Unlike our meshes of the Carleson quadrilaterals and right pentagons, our mesh of the Carleson triangles will use the full interval of angles  $[60^\circ, 120^\circ]$ . This is easy to do if we just want to mesh by quadrilaterals with circular arc sides. However, we will want to conformally map our mesh in  $\mathbb{D}$  to  $\Omega$  and then replace the curved edges in the image by straight line segments. This can change the angles slightly, so we would end up with angles in  $[60^\circ - \epsilon, 120^\circ + \epsilon]$  (where  $\epsilon$  depends on the ratio between the diameters of our mesh elements and the diameter of  $T$ ). To get the sharp result, we will have to be careful how we use angles near  $60^\circ$  and  $120^\circ$ . To simplify matters, it will be enough to simply consider one special Carleson triangle  $T$  in the upper half-plane model with vertices at  $-1, 1, i/(\sqrt{2} - 1)$ . The mesh for any other triangle will be obtained as a Möbius image of the mesh we construct on this triangle.

The triangle  $T$  has one vertex in  $\mathbb{H}$ , and we refer to this as the “top point”. Adjacent to the top point are two sides that we call the “left” and “right” sides. Inside  $T$  we will construct an “inner triangle”  $T_i \subset T$ . The vertices of  $T_i$  form an ordinary equilateral Euclidean triangle, but the edges of  $T_i$  itself are circular arcs meeting at three interior angles of  $90^\circ$ , and  $T_i$  is uniquely determined by this.

**Lemma 6.1.** *The following holds for all sufficiently large integers  $N$ . There is a sequence  $d_1 < d_2 < \dots < d_M$  with  $|d_k - d_{k+1}| \leq 1/N$  for  $k = 1, \dots, M - 1$  and a mesh of  $T$  into hyperbolic quadrilaterals with angles between  $60^\circ$  and  $120^\circ$  so that the vertices along the left and right edges of  $T$  occur exactly at the points distance  $d_k$ ,  $k = 1, \dots, m$  from the top point. Every quadrilateral  $Q$  in the mesh satisfies  $\text{diam}(Q) = O(\frac{1}{N} \cdot \text{diam}(T))$ . The triangle  $T$  contains a symmetric right circular triangle  $T_i \subset T$  so that outside  $T_i$ , only angles in  $[90^\circ - O(\frac{1}{N}), 90^\circ + O(\frac{1}{N})]$  are used. The triangle  $T_i$  may be chosen as small as wish compared to  $T$ . Replacing edges by straight line segments gives angles between  $60^\circ$  and  $120^\circ$ .*

The inner triangle  $T_i$  is divided into three quadrilaterals by connecting the center of the triangle to the midpoint of each edge by a straight line. The vertices of  $T_i$  and the midpoints of its edges are connected to points on  $\partial T$  by circular arcs that are perpendicular to the both the boundaries of  $T$  and  $T_i$  at the points where they meet. See Figure 10. We mesh each of the nine resulting quadrilaterals using the foliations

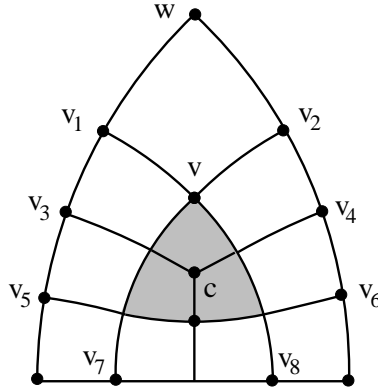


FIGURE 10. The outer triangle  $T$  is a Carleson triangle in the upper half-plane with top point  $w = i/(\sqrt{2} - 1)$ . Its interior is divided into an inner triangle  $T_i$  (shaded) with top point  $v$  and nine surrounding right circular quadrilaterals. The points  $v_1, v_2$  are equidistant from  $w$  in the hyperbolic metric. The left and right sides of  $T_i$  are geodesic segments and extend to hit  $\mathbb{R}$  as points  $v_7, v_8$ . The Carleson triangle with vertices  $v, v_7, v_8$  is denoted  $T_e$ .

given in Lemma 5.2, starting at the left and right sides of  $T$  at the points given by  $\{d_k\}$ . We assume that this collection contains the distances  $\rho(w, v_1), \rho(w, v_3), \rho(w, v_5)$ . When a leaf ends we continue it in the next quadrilateral (assume we know how to do this for the inner triangle and that the foliation there is symmetric). The path continues until it either it hits  $c$  (the center of the inner triangle), hits  $[-1, 1]$  (the base of  $T$ ) or hits the opposite side of  $T$ . In the latter case, symmetry implies the path ends at a point the same distance from the top point as its starting point.

The choice of inner triangle  $T_i$  depends only on the choice of its top point. This lies on the positive imaginary axis, and  $T_i$  is chosen to be symmetric with respect to this line. The diameter of  $T_i$  is scaled so that the left and right edges of  $T_i$  are hyperbolic geodesic segments (if the top point has height  $h$  above 0, the three vertices of  $T_i$  should form an equilateral triangle of sidelength  $h(\sqrt{3} - 1)$ ; see Figure 11). Since any point between the top point of  $T$  and the origin can be used, the inner triangle can be as small as we wish.

We define three foliations on this triangle  $T_i$ . For each vertex  $v$ , reflect  $v$  through the circular arc on the opposite side to define a point  $v^*$  and foliate  $T_i$  by arcs that lie on circles passing through both  $v$  and  $v^*$ . Note that each foliation leaf passes through one of the vertices of  $T_i$  and is perpendicular to the opposite side. See Figure 12. The

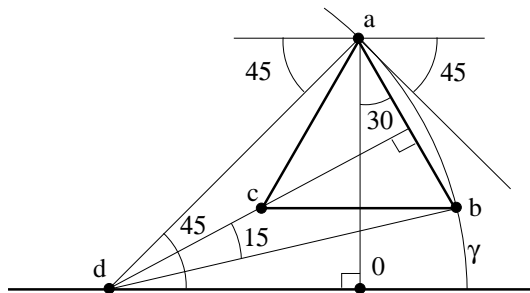


FIGURE 11. How to scale the inner triangle. Suppose  $a$  is height 1 above the real axis and  $a, b$  lie on a geodesic  $\gamma$  centered at  $d$  that makes a  $45^\circ$  angle with the horizontal at  $a$ . The  $\Delta a0d$  is isosceles with base angles  $45^\circ$ , so  $|ad| = |bd| = \sqrt{2}$ . The line  $da$  is perpendicular to  $\gamma$ , so  $\Delta dab$  is isosceles. Thus  $|ab| = 2|bd| \sin(15^\circ) = \sqrt{3} - 1$ .

center of the triangle can be connected to the midpoint of each side by a foliation leaf that is a straight line, dividing  $T$  into three quadrilaterals. Restrict each foliation to the two quadrilaterals that are not adjacent to the vertex it passes through. This gives two foliations on each quadrilateral. See Figure 12. Taking a finite set of leaves for each foliation gives a quadrilateral mesh of the right circular triangle.

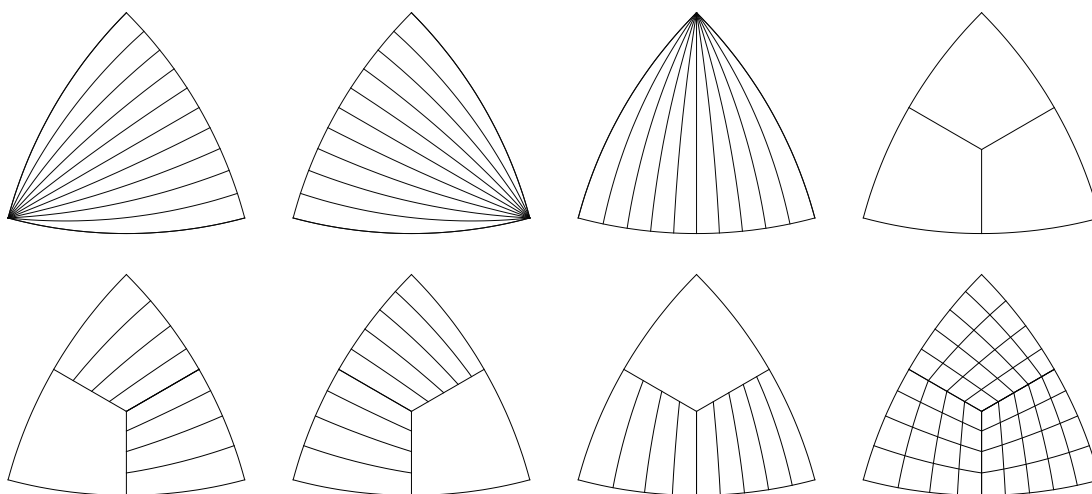


FIGURE 12. Three foliations of a circular right triangle. Each leaf passes through an associated vertex and is perpendicular to the opposite side. Connecting the center of the triangle to the midpoints of each side by the straight leaf divides  $T_i$  into three quadrilaterals. We then restrict each foliation to two of the quadrilaterals as shown, and leaves of the union give the mesh edges.

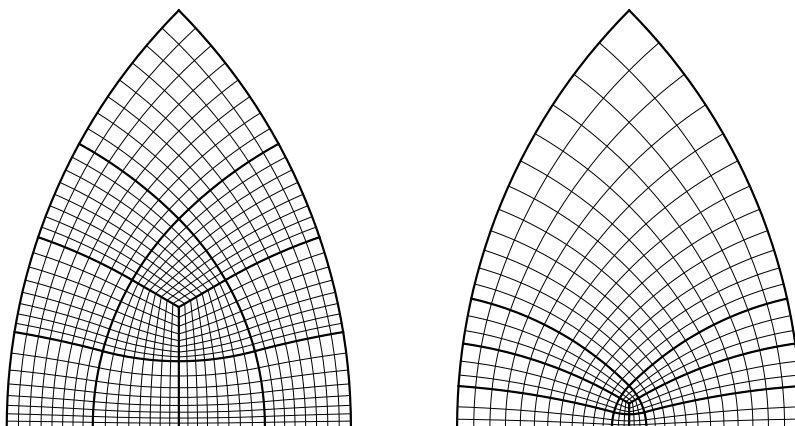


FIGURE 13. The mesh of a Carleson triangle for two different positions of the inner triangle.

Combining this foliation of the inner triangle with the foliations of the surrounding quadrilaterals and choosing starting points along the left and right sides of  $T$  as described earlier gives the desired mesh of  $T$ . See Figure 13. The only part of the lemma left to prove is the claim that the angle are in the desired interval when replace the curved edges by straight segments.

When we replace the circular arc edges in the mesh by straight line segments, It is not obvious that they all remain in  $[60^\circ, 120^\circ]$ , but we will show that this is true. Consider a point  $z$  in one of the three quadrilaterals and the two foliation paths  $\gamma_1, \gamma_2$  that connect it to the two opposite vertices,  $v_1, v_2$  respectively. See Figure 14. Let  $L_1, L_2$  be the lines through the center  $c$  and the points  $v_1, v_2$ . If we think of the arc  $\gamma_1$  as a graph over the line  $L_1$  it is monotonically increasing as we move away from  $v_1$  and remains increasing so as long as we stay inside the triangle (since  $\gamma_1$  is perpendicular the the opposite side of the triangle, the point of greatest distance from  $L_1$  occurs outside the triangle). Thus if we translate  $L_1$  to pass through the point  $z$ , we see that  $\gamma_1$  stays on one side of this new line up to  $z$  and on the other side beyond  $z$ . Thus any chord of  $\gamma_1$  in the triangle with one endpoint at  $z$  also stays on the same side of the line as the corresponding arc of  $\gamma_1$ . Similar for  $\gamma_2$  and  $L_2$ . See the right side of Figure 14. Thus if we replace foliation paths by segments, at each vertex there will be two angles less than  $120^\circ$  and two greater than  $60^\circ$  (which are the angles formed by  $L_1$  and  $L_2$ ). This completes the proof of Lemma 6.1.

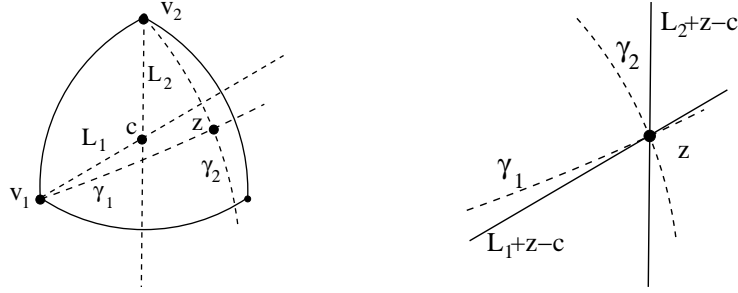


FIGURE 14. If we choose any point  $z$  of the equilateral triangle then chords of the foliation paths with endpoint  $z$  form angles that are bounded between  $60^\circ$  and  $120^\circ$ .

## 7. MESHING THE THICK PARTS BY CONFORMAL MAPS

The Riemann mapping theorem says that given any simply connected planar domain  $\Omega$  (other than the whole plane) there is a 1-1, onto, holomorphic map of the disk onto  $\Omega$ . Moreover, we may map 0 to any point of  $\Omega$  and specify the argument of the derivative at 0. Such a mapping is conformal, i.e., it preserves angles locally. More importantly, a conformal mapping is close to linear on small balls with estimates that depend on the ball but not on the mapping. Koebe's estimate (e.g. Cor. 4.4 of [10]) says that if  $f : \mathbb{D} \rightarrow \Omega$  is conformal then

$$\frac{1}{4}|f'(z)| \leq \frac{\text{dist}(z, \partial\Omega_1)}{\text{dist}(f(z), \partial\Omega_2)} \leq |f'(z)|.$$

The closely related distortion theorem states (Equation (4.17) of [10]) that if  $f$  is conformal on the unit disk, then

$$\frac{1 - |z|}{(1 + |z|)^2} \leq \frac{|f'(z)|}{|f'(0)|} \leq \frac{1 + |z|}{(1 - |z|)^3},$$

This says that on small balls  $f'$  is close to constant, and hence that  $f$  is close to linear. More precisely, if  $f$  is conformal on a ball  $B(w, r)$  then

$$(7.1) \quad |f(z) - L(z)| \leq O(\epsilon^2 |f'(z)| r),$$

for  $z \in B(w, \epsilon r)$ , where  $L(z) = f(w) + (z - w)f'(w)$  is a Euclidean similarity.

We are particularly interested in conformal maps onto polygons. In this case  $f$  is given by the Schwarz-Christoffel formula

$$g(z) = A + C \int \prod_{k=1}^{n-1} (w - z_k)^{\alpha_k - 1} dw,$$

where the interior angles of  $\Omega$  are  $\{\alpha_1\pi, \dots, \alpha_n\pi\}$  and the preimages of the vertices are  $\mathbf{z} = \{z_1, \dots, z_n\}$ . See e.g., [8], [12], [16]. The formula was discovered independently by Christoffel in 1867 [7] and Schwarz in 1869 [14], [13]. For other references and a brief history see Section 1.2 of [8]. The difficulty in using the formula is to find the correct parameters  $\mathbf{z}$  for a given  $\Omega$ .

For a conformal map  $f$  onto a polygonal region, the points of the prevertex set  $\mathbf{z} \subset \mathbb{T}$  are the only singularities of  $f$  on  $\mathbb{T}$ . The map extends analytically across the complementary intervals by the Schwarz reflection theorem. Thus for a point  $w \in \mathbb{D}$ , the map  $f$  extends to be conformal on the ball  $B = B(w, \text{dist}(w, E))$ , and if  $Q \subset B$  and  $\text{diam}(Q) \leq \epsilon \cdot \text{dist}(Q, E)$ , then there is a linear map  $L$  so that

$$(7.2) \quad |f(z) - L(z)| \leq O(\epsilon \text{diam}(f(Q))),$$

for  $z \in Q$ . In particular, the images of the vertices of  $Q$  map to the vertices of a quadrilateral whose angles differ by only  $O(\epsilon)$  from the angles of  $Q$ . This is what allows us to map our mesh via a conformal map and obtain a mesh with only slightly distorted angles. More precisely,

**Lemma 7.1.** *Suppose  $f : \mathbb{D} \rightarrow \Omega$  is a conformal map onto a polygonal domain with singular set  $\mathbf{z}$  and  $Q \subset \mathbb{D}$  is a Euclidean quadrilateral with  $\text{diam}(Q) \leq \epsilon \cdot \text{dist}(Q, \mathbf{z})$ . Then the images of the vertices of  $Q$  under  $f$  form a quadrilateral with angles differing by at most  $O(\epsilon)$  from the corresponding angles of  $Q$ .*

If we applied this directly to a general polygonal region we could prove that there is a quadrilateral mesh with angles between  $60^\circ - O(\epsilon)$  and  $120^\circ + O(\epsilon)$  for any  $\epsilon > 0$ , but we would not have the  $O(n)$  bound on the number of pieces. Bounding the number of terms comes from using a special decomposition of  $\Omega$  and getting rid of the  $\epsilon$ 's comes from modifying the conformal map near the inner triangles in our mesh of  $\mathbb{D}$ . We will deal with the decomposition first.

A polygonal domain  $\Omega$  is  $\delta$ -thick if the corresponding prevertex set  $\mathbf{z}$  is  $\delta$ -thick, as defined in Section 2. Equivalently, any two non-adjacent sides of  $\Omega$  have extremal distance at least  $\delta$  in  $\Omega$ . Extremal distance is a well know conformal invariant which roughly measures the distance between two continua compared to their diameters. For more details about extremal distance and thick domains, see [6].

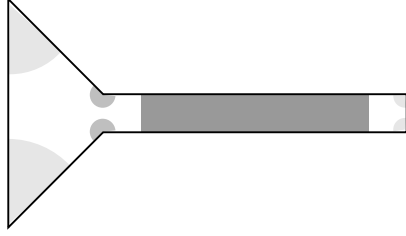


FIGURE 15. A polygon with one hyperbolic thin part (darker) and six parabolic thin parts.

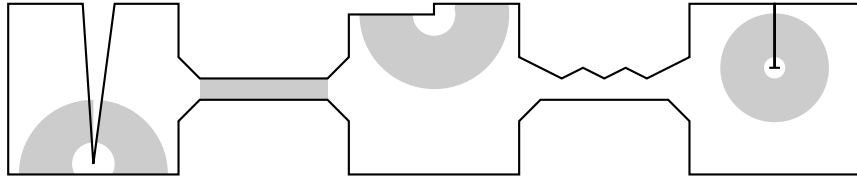


FIGURE 16. A polygon with five hyperbolic thin parts. This figure is not to scale. The channel on the right is not thin because the upper edge is made up of numerous short edges; the extremal distance from any of these to the lower edge is bounded away from zero.

A subdomain  $\Omega' \subset \Omega$  is  $\delta$ -thin if (1)  $\partial\Omega' \cap \partial\Omega$  consists of two segments  $S_1, S_2$  (each a subset of distinct edges of  $\Omega$ ), (2)  $\partial\Omega' \cap \Omega$  consists of two polygonal arcs, each inscribed in an approximate circle and (3) the extremal distance between  $S_1$  and  $S_2$  in  $\Omega'$  is  $\leq \delta$ . A thin part of  $\Omega$  is called parabolic if the sides  $S_1, S_2$  lie on adjacent sides of  $\Omega$  is called hyperbolic otherwise. See Figures 15 and 16. The following result is proven in [6].

**Lemma 7.2.** *There is an  $\delta_0 > 0$  and  $0 < C < \infty$  so that if  $\delta < \delta_0$  then the following holds. Given a simply connected, polygonal domain  $\Omega$  we can write  $\Omega$  is a union of subdomains  $\{\Omega_j\}$  belonging to two families  $\mathcal{N}$  and  $\mathcal{K}$ . The elements of  $\mathcal{N}$  are  $O(\delta)$ -thin polygons and the elements of  $\mathcal{K}$  are  $\delta$ -thick. The number of edges in all the pieces put together is  $O(n)$  and all the pieces can be computed in time  $O(n)$  (constant depends on  $\epsilon$ ). A piece can only intersect a piece of the opposite type. Any such intersection is a  $4\delta$ -thin polygon.*

Suppose  $\Omega_1$  is one of the thick parts, and let  $f : \mathbb{D} \rightarrow \Omega_1$  be a conformal map with the origin mapping to a point outside of all the thin parts hitting  $\Omega_1$ . Note that

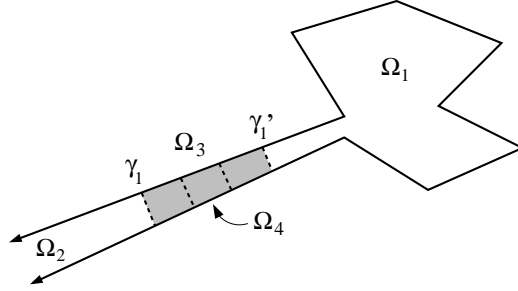


FIGURE 17. An overlapping thick piece,  $\Omega_2$ , and thin piece,  $\Omega_1$  and crosscuts  $\gamma_1 = \partial\Omega_1 \cap \Omega_2$ ,  $\gamma_2 = \partial\Omega_2 \cap \Omega_1$ . The shaded region is  $\Omega_3 = \Omega_1 \cap \Omega_2$ . This region is divided into three sections and in the center section is denoted  $\Omega_4$ .

$\partial\Omega_1 \cap \Omega$  consists of crosscuts  $\{\gamma_j\}$  and let  $\{I_j\}$  be the preimages under  $f$  of these boundary arcs. Each  $\gamma_j$  has an associated crosscut  $\gamma_j'$  that is a boundary arc of the thin part containing  $\gamma_j$ . The preimage of  $\gamma_j'$  defines a crosscut in  $\mathbb{D}$  whose endpoints define an interval that contains  $AI_j$  of  $I_j$  where  $A \simeq \exp(\pi/4\delta)$ . These larger intervals are disjoint (since none of the thin parts intersect) and  $f(0)$  can be chosen so they all have length  $< \pi$ .

Thus we can apply Lemma 3.2 to construct a domain  $W_1 \subset \mathbb{D}$  and a quadrilateral mesh on it. Suppose  $\partial\Omega_1$  has  $n_1$  sides. Since  $\Omega_1$  is  $\delta$ -thick, Lemma 3.3 implies the mesh of  $W_1$  has  $O(n_1)$  elements, with a constant depending on  $\delta$ . Moreover, for any  $\epsilon > 0$  we may assume Lemma 7.1 applies to all the quadrilaterals in our mesh of  $W_1$  if we take  $\epsilon = O(1/N)$  where  $N$  is in Lemmas 4.1, 5.1 and 6.1). Thus  $f(W_1) \subset \Omega_1$  has a mesh with  $O(n_1)$  quadrilaterals, the constant depending on  $\delta$  and  $N$ , which we will choose independent of  $\Omega$ . If  $N$  is large enough, then all angles are in the desired range, except possibly for the quadrilaterals corresponding to the inner triangles. This determine the choice of  $N$ .

We also want to choose  $\delta > 0$  independent of  $\Omega$ . As above, suppose  $\Omega_1$  is a thick piece and that it intersects a thin piece  $\Omega_2$ . The intersection,  $\Omega_3 = \Omega_1 \cap \Omega_2$  is a  $4\delta$ -thin part and can be divided into three disjoint  $12\delta$ -thin parts as illustrated in Figure 17. Let  $\Omega_4$  denote the “middle” part (the one separated from both  $\gamma_1$  and  $\gamma_2$ ). For points inside  $\Omega_4$ , the conformal maps of the disk to  $\Omega_1$  and  $\Omega_3$  are very close to each other if  $\delta$  is small enough. The following result (Lemma 24 of [6]) makes this precise:

**Lemma 7.3.** *Suppose  $f : \mathbb{H} \rightarrow \Omega_1$  is conformal. We can choose a conformal map  $g : \mathbb{H} \rightarrow \Omega_3$  so that for  $z \in f^{-1}(\Omega_4)$ , and uniform  $c > 0, C < \infty$ ,*

$$|f(z) - g(z)| \leq C \exp(-c/\delta) \max(\text{diam}(\gamma_1), \text{diam}(\gamma_2)).$$

Since  $\Omega_3$  is a thin part, we can renormalize our maps so that  $f(i) = g(i)$  is the center of  $\Omega_4$  and the preimages of the vertices of  $\Omega_3$  under  $g$  can be grouped into two parts: those in a small interval  $\{|x| < \eta\}$  and those outside a large interval  $\{|x| > 1/\eta\}$ , where  $\eta$  tends to zero as  $\delta$  tends to zero.

The corresponding terms of the Schwarz-Christoffel formula can be grouped as

$$g'(w) = B \prod_{|z_k| < \eta} w^{\alpha_k - 1} \left(1 - \frac{z_k}{w}\right)^{\alpha_k - 1} \prod_{|z_j| > 1/\eta} \left(1 - \frac{w}{z_j}\right)^{\alpha_j - 1} \simeq B w^{\sum_{k: |z_k| < \eta} \alpha_k - 1} = B w^\beta,$$

where  $B$  is constant, and the dropped terms are close to 1 if  $\eta$  is close to 0. Thus  $g$  approximates a power function. This implies that  $g$ , and hence  $f$ , maps the circular arc  $\{|z| = 1\} \cap \mathbb{H}$  to a smooth crosscut of  $\Omega_4$  that approximates a circular arc that is close to perpendicular to the boundary, and that  $f$  followed by radial projection onto this arc preserves the ordering of points and multiplies the distances between them by approximately a constant factor (with error that tends to zero with  $\delta$ ). Figure 18. This is one condition that determines our choice of  $\delta$ . Another will be given in the final section when we mesh hyperbolic thin parts.

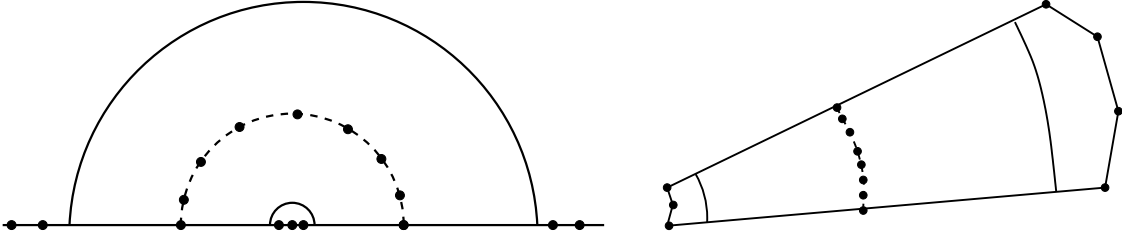


FIGURE 18. Inside the middle of the overlap of a thick and thin part, the conformal map approximates a power function. Points on a circular arc in the disk are mapped to points that lie on an approximate circular arc and order is preserved.

We now transfer the mesh from  $W_1$  to  $f(W_1) \subset \Omega_1$ . The unmeshed portions of  $\Omega$  are now all subsets of thin parts bounded by crosscuts that are almost circular arcs. Moreover, the number of mesh vertices on each of these crosscuts is the same by (3) of Lemma 3.2 (namely  $3N + 2M$  where  $N$  is from Lemma 4.1 and  $M$  is from Lemmas

5.1 and 6.1). The mesh has all angles in  $[60^\circ, 120^\circ]$ , except those corresponding to the inner triangles in the Carleson triangles, where they may be  $O(\epsilon)$  larger or smaller.

To fix this, we replace the conformal map by a linear map in the inner triangles. Map each Carleson triangle in  $\mathbb{D}$  used in the mesh of  $W_1$ , to the Carleson triangle  $T$  in  $\mathbb{H}$  discussed in Section 6 using a Möbius transformation  $\tau$ . Then  $g = f_k \circ \tau^{-1}$  is a conformal map of  $T$  into a part of  $f(W_1)$  and we transfer our mesh of  $T$  outside the inner triangle  $T_i$  via this map. This agrees with our previous definition. In the inner triangle  $T_i$  we use the linear map  $h(z) = g(c) + (z - c)g'(c)$  to transfer the mesh. This preserves angles exactly and so the image quadrilaterals have angles in  $[60^\circ, 120^\circ]$ . For quadrilaterals along the boundary of  $T_i$  we apply  $h$  to the vertices on  $\partial T_i$  and  $g$  to the vertices in  $T \setminus T_i$ . Along the boundary of  $T_i$ ,  $|h(z) - g(z)| = O(\eta^2)\text{diam}(g(T_i))$  where  $\eta = \text{diam}(T_i)/\text{dist}(T_i, \mathbf{z}) = O(\text{diam}(T_i)/\text{diam}(T))$ . Since the quadrilaterals meshing  $T$  along  $\partial T_i$  have Euclidean diameter  $\simeq \eta$ , and angles all near  $90^\circ$ , we see that the angles of the image quadrilaterals also have angles near  $90^\circ$  if  $\eta$  is small enough, i.e., if the inner triangle is small enough with respect to the outer triangle. This determines the choice of the inner triangle.

This completes the proof that the desired mesh exists, except for meshing the thin parts, which is done in the next section. However, this is not quite a linear time algorithm for computing the mesh, since we have used evaluations of conformal maps without an estimate of the work involved. We address this now.

The exact conformal map onto a general polygon probably can't be computed in finite time, but we can compute an approximate map onto a simple  $n$ -gon in time  $O(n)$  with a constant depending only on the desired accuracy. In [6] I show that a  $(1 + \epsilon)$ -quasiconformal map from  $\mathbb{D}$  to  $\Omega$  can be computed and evaluated at  $n$  points in time  $O(n)$  where the constant depends only on  $\epsilon$ . I will refer to [6] for the definition and relevant properties of quasiconformal mappings, but the point is that if  $f : \mathbb{D} \rightarrow \Omega$  is conformal and  $g : \mathbb{D} \rightarrow \Omega$  is the  $(1 + \epsilon)$ -quasiconformal approximation constructed in [6], and if we have a Euclidean quadrilateral  $Q$  in our mesh, then the  $g$ -images of the vertices of  $Q$  give angles that are  $O(\epsilon)$  close to the angles in the  $f$  image. Thus using  $g$  to transfer the mesh vertices works just as well as  $f$ . The fast Riemann mapping theorem given in [6] implies:

**Theorem 7.4.** *Suppose we are given a thick simply connected region  $\Omega$  bounded by a simple  $n$ -gon and an  $\epsilon > 0$ . We can compute the thick/thin decomposition of  $\Omega$ , the corresponding domain  $W$  and its quadrilateral mesh and a map  $g$  on vertices of the mesh that extends to a  $(1 + \epsilon)$ -quasiconformal map of the disk to  $\Omega$ . The total work is  $O(n)$  where the constant may depend on  $\epsilon$ .*

In fact, we do not need the full strength of the result in [6], giving the dependence on  $\epsilon$ , since we only need to apply the result for a small, but fixed,  $\epsilon$ . Moreover, we only need the result for thick polygons, which is an easier case of the theorem.

## 8. MESHING THE THIN PARTS

We are now done with the proof of Theorem 1.1 except for meshing thin parts. Each such thin part is either bounded by two adjacent edges of  $\Omega$  and an almost circular crosscut  $\gamma$  (the parabolic case) or by two non-adjacent edges and two almost circular crosscuts  $\gamma_1, \gamma_2$  (the hyperbolic case).

We start with parabolic thin parts where the two adjacent edges of  $\Omega$  meet at vertex  $v$  with angle  $\theta \leq 120^\circ$ . The crosscut  $\gamma$  defines a neighborhood of  $v$  in  $\Omega$  that is approximately a sector, and we define a true circular sector  $S$  with vertex  $v$  of comparable, but smaller, size. See Figure 19. This sector is divided into pieces using circular arcs concentric with  $v$  and radial segments, as shown in the left of Figure 19. There are several levels, with the width of the level decreasing by a factor of 2 as we move away from  $v$ , and we split each level with radial segments in order to increase the number of vertices on the outer edge of the sector. This can be done so that if we divide  $S$  into four equal sectors (each of angle  $\theta/4 \leq 30^\circ$ ) and add extra vertices to the centers of some arcs, then the number of points on the outer edge in each subsector is the same as the number of vertices on  $\gamma$  in the same subsector.

If we list the points on  $\gamma$  and on the outer edge of the sector in order, then corresponding points lie in the same subsector and can be joined by segments that make angle between  $90^\circ - \theta/2 - \epsilon \geq 75^\circ - \epsilon$  and  $105^\circ + \epsilon$  with the chords of the outer edge of the sector. See Figure 20. A similar estimate holds for the chords on  $\gamma$  (with a larger  $\epsilon$  since  $\gamma$  is only an approximate circle). Here  $\epsilon$  tends to zero as  $S$  shrinks with respect to  $\gamma$ . We simply choose a relative size for  $S$  that causes these angles to be between  $60^\circ$  and  $120^\circ$ .

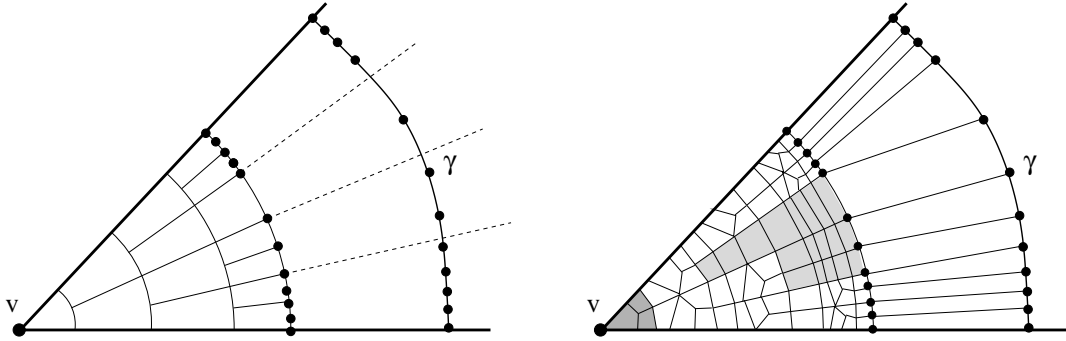
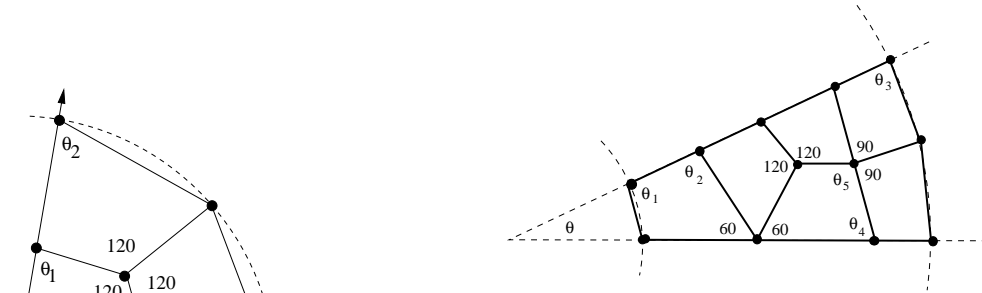


FIGURE 19. The crosscut  $\gamma$  defines a neighborhood of the vertex  $v$ . We define a sector of comparable size and partition the sector, so that the number of vertices on the outer edge approximates the number of points on the crosscut  $\gamma$ . The pieces are then meshed: Mesh 1 is used in dark shaded region, Mesh 2 (or its reflection) the white regions and segments only in the lighter shaded regions. The number of vertices on the outer edge is exactly the number on  $\gamma$  and corresponding points are joined by segments.



Mesh 1

$$\begin{aligned}
 &0 < \theta \leq 120 \\
 &60 \leq \theta_1 = 180 - 60 - \frac{1}{2}\theta \leq 120 \\
 &60 \leq \theta_2 = \frac{1}{2}(180 - \frac{1}{2}\theta) \leq 90
 \end{aligned}$$

Mesh 2

$$\begin{aligned}
 &0 \leq \theta \leq 60 \\
 &90 \leq \theta_1 = 180 - \frac{1}{2}(180 - \theta) \leq 120 \\
 &60 \leq \theta_2 = 360 - 60 - 2\theta_1 \leq 120 \\
 &75 \leq \theta_3 = 90 - \frac{1}{4}\theta \leq 90 \\
 &60 \leq \theta_4 = 90 - \frac{1}{2}\theta \leq 90 \\
 &90 \leq \theta_5 = 360 - 120 - 60 - \theta_4 \leq 120
 \end{aligned}$$

We then have to mesh  $S$  so that the mesh vertices on the outer edge are exactly the ones given above. We do this by applying the illustrated constructions in each

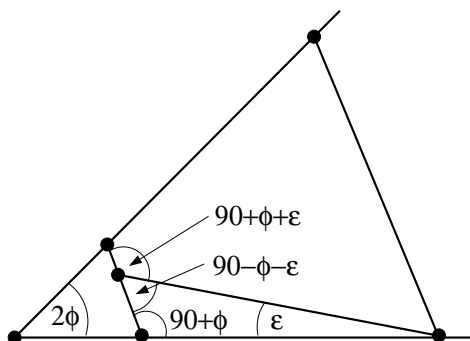


FIGURE 20. The connecting segments between  $\gamma$  and the outer edge of  $S$  lie inside a sector of angle  $2\phi \leq 30$ . If the  $S$  is small enough compared to  $\gamma$  the angle marked  $\epsilon$  is as small as we wish, say  $\epsilon < 10^\circ$ . Then the angles formed with the chords of the outer edge of  $S$  are between  $65^\circ$  and  $115^\circ$ . The angles with the chords along  $\gamma$  are slightly smaller/larger since  $\gamma$  is only an approximate circle, but the difference is as small as wish by taking the parameter  $\delta$  in our thick/thin decomposition small enough.

part of the sector. Mesh 1 is used only in the piece adjacent to  $v$  and the equations below the figure show that all the new angles are in the correct range. Mesh 2 (or its reflection) are used in all the pieces that have one more vertex on their outer edge than on the inner edge (we use reflections to make the vertices on the radial edges match up). Otherwise we simply use chords of circles concentric with  $v$  to connect edge vertices of parts where mesh 2 was used. See the right side of Figure 19.

If the interior angle at  $v$  is  $120^\circ \leq \theta < 240^\circ$  then we bisect the angle as part of our partition of the sector. If  $240^\circ \leq \theta \leq 360^\circ$ , then we trisect the angle. See Figure 21.

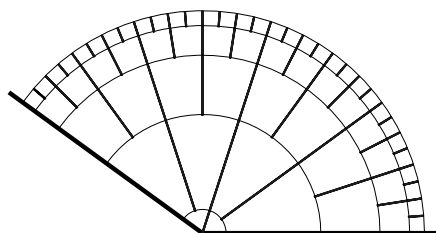


FIGURE 21. If the vertex has interior angle between  $120^\circ$  and  $240^\circ$  then we bisect the angle as part of the sector partition and mesh each piece as before.

A hyperbolic thin part is bounded by two straight line segments in  $\partial\Omega$  and two almost circular crosscuts  $\gamma_1, \gamma_2$ . Both crosscuts contain the same number,  $P$ , of vertices from the meshes of the corresponding thick pieces. If the two straight sides are parallel or lie on lines that intersect with small angle, then just connecting each point on  $\gamma_1$  to the corresponding point on  $\gamma_2$  will give angles in the desired range. In general, however, this is not the case, but is easily fixed by adding a bounded number of circular crosscuts separating  $\gamma_1, \gamma_2$  and using a polygonal chain with vertices on these crosscuts to connect each vertex on  $\gamma_1$  to the corresponding vertex on  $\gamma_2$ . It is easy to see that this can be done with angles close to  $90^\circ$  if the number of intermediate crosscuts is large enough and  $\delta$  (the degree of thinness) is small enough. See Figure 22. This places an additional constraint on the choice of  $\delta$ .

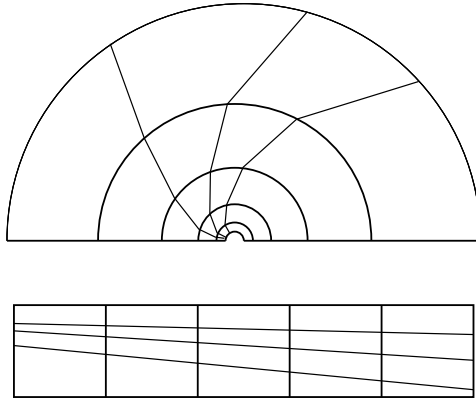


FIGURE 22. By adding a bounded number of circular crosscuts to a hyperbolic thin part we can connect any  $P$  points on  $\gamma_1$  to any  $P$  points on  $\gamma_2$  with a mesh using angles near  $90^\circ$ . The arcs look like logarithmic spirals. Indeed, we can think of this mesh as approximating the image of the lower picture under the complex exponential map.

In addition to the angle bounds, every quadrilateral in the construction can be chosen to have bounded geometry (i.e., all four edges of comparable length with uniform constants) except in two cases. First, when we mesh a parabolic thin part with angle  $\theta \ll 1$ , the piece containing the vertex has two sides with length only  $O(\theta)$  as long as the other two. Second, when meshing a hyperbolic thin part we use long, narrow pieces, but if the long sides have extremal distance  $\delta$ , we can refine the mesh by subdividing each such piece into  $O(1/\delta)$  bounded geometry quadrilaterals. Thus if the hyperbolic thin parts of  $\Omega$  have “thinnesses”  $\{\delta_k\}$ , then we can mesh  $\Omega$

by  $O(n + \sum_k \delta_k^{-1})$  quadrilaterals with angles in  $[60^\circ, 120^\circ]$  and bounded geometry, except for the pieces containing vertices with small angles. If  $\Omega$  has no small angles, this gives the smallest (up to a constant factor), bounded geometry mesh of  $\Omega$ .

## REFERENCES

- [1] A.F. Beardon. *The geometry of discrete groups*. Springer-Verlag, New York, 1983.
- [2] M. Bern and D. Eppstein. Quadrilateral meshing by circle packing. *Internat. J. Comput. Geom. Appl.*, 10(4):347–360, 2000. Selected papers from the Sixth International Meshing Roundtable, Part II (Park City, UT, 1997).
- [3] C.J. Bishop. Divergence groups have the Bowen property. *Ann. of Math. (2)*, 154(1):205–217, 2001.
- [4] C.J. Bishop. Quasiconformal Lipschitz maps, Sullivan’s convex hull theorem and Brennan’s conjecture. *Ark. Mat.*, 40(1):1–26, 2002.
- [5] C.J. Bishop. An explicit constant for Sullivan’s convex hull theorem. In *In the tradition of Ahlfors and Bers, III*, volume 355 of *Contemp. Math.*, pages 41–69. Amer. Math. Soc., Providence, RI, 2004.
- [6] C.J. Bishop. Conformal mapping in linear time. 2006. Preprint.
- [7] E.B. Christoffle. Sul problema della temperatura stazonaire e la rappresetazione di una data superficie. *Ann. Mat. Pura Appl. Serie II*, pages 89–103, 1867.
- [8] T.A. Driscoll and L.N. Trefethen. *Schwarz-Christoffel mapping*, volume 8 of *Cambridge Monographs on Applied and Computational Mathematics*. Cambridge University Press, Cambridge, 2002.
- [9] D.B.A. Epstein and A. Marden. Convex hulls in hyperbolic space, a theorem of Sullivan, and measured pleated surfaces. In *Analytical and geometric aspects of hyperbolic space (Coventry/Durham, 1984)*, volume 111 of *London Math. Soc. Lecture Note Ser.*, pages 113–253. Cambridge Univ. Press, Cambridge, 1987.
- [10] J.B. Garnett and D.E. Marshall. *Harmonic measure*, volume 2 of *New Mathematical Monographs*. Cambridge University Press, Cambridge, 2005.
- [11] J. L. Gerber. The dissection of a polygon into nearly equilateral triangles. *Geom. Dedicata*, 16(1):93–106, 1984.
- [12] Z. Nehari. *Conformal mapping*. Dover Publications Inc., New York, 1975. Reprinting of the 1952 edition.
- [13] H.A. Schwarz. Confome abbildung der oberfläche eines tetraeders auf die oberfläche einer kugel. *J. Reine Ange. Math.*, pages 121–136, 1869. Also in collected works, [14], pp. 84-101.
- [14] H.A. Schwarz. *Gesammelte Mathematische Abhandlungen*. Springer, Berlin, 1890.
- [15] D. Sullivan. Travaux de Thurston sur les groupes quasi-fuchsien et les variétés hyperboliques de dimension 3 fibrées sur  $S^1$ . In *Bourbaki Seminar, Vol. 1979/80*, pages 196–214. Springer, Berlin, 1981.
- [16] L. N. Trefethen and T.A. Driscoll. Schwarz-Christoffel mapping in the computer era. In *Proceedings of the International Congress of Mathematicians, Vol. III (Berlin, 1998)*, number Extra Vol. III, pages 533–542 (electronic), 1998.

C.J. BISHOP, MATHEMATICS DEPARTMENT, SUNY AT STONY BROOK, STONY BROOK, NY 11794-3651

*E-mail address:* bishop@math.sunysb.edu